Numerical Modelling and Analysis on the Behaviour of GFRP Pultruded I Beams Strengthened with CFRP Laminates

G.Ganesan[A], Research Scholar, Department of Civil and Structural Engineering, Annamalai University, Annamalai Nagar, Tamil Nadu, India,

Dr.G.Kumaran[B], Professor, Department of Civil and Structural Engineering, Annamalai University, Annamalai Nagar, Tamil Nadu, India,

Abstract: This paper presents the numerical and experimental characterization of the behaviour of GFRP pultruded profiles strengthened with CFRP laminates. The static behaviour of these hybrid beams are studied by conducting four-point and three-point bending tests. CFRP laminates of different orientation and different thickness are used for strengthening. The results of the test acquired showed that strengthening by CFRP laminates increases the load bearing ability as well as, can control the deflection. A linear relationship was exhibited in Moment Vs Curvature, of the test beams. A static non-linear analysis is carried to develop reliable and computationally competent finite element models for the analysis of FRP Pultruded I-beams under two point loading conditions. This model developed in this study is used to replicate the static experimental tests which are performed. The results acquired through the experimental study have good accord with those obtained from the finite element analysis.

Keywords —Flexural stiffness, Glass fibre reinforced Plastic, Numerical modeling, Pultruded Profiles.

I. INTRODUCTION

In construction industry, the use of FRP pultruded profiles, have gained wide application, due to their advantages like light weight, high strength, resistance to corrosion etc. Recently, they are widely being used in the building of bridge systems, walkways and other structures exposed to corrosive.

GFRP profiles are commonly used in construction industry due to many advantages, like light weight, anti-corrosive, etc. The design of GFRP profiles is influenced by the restrictions in deflection at service loads or by buckling, in case of thin walled sections, because of the relatively low elastic moduli. To overcome these effects, CFRP laminates were used to reinforce the profiles.

The laminate of different fibre orientation of advanced composite resources may display complex anisotropic behaviour. It is generally accepted that for profiles fabricated by the Pultrusion profiles, the section walls can be assumed as laminated composites with same orthotropic mechanical properties in both, longitudinal and transverse directions. While changes in the profile section geometry are easily related to changes in the stiffness, changes in the material and fibre orientation are not so obvious to be evaluated. **Bank(1989)[1]** has shown that, due the dissimilarities in mechanical properties between a full size profile of thin walled section and a solid bar of rectangular piece, the modulus of elasticity in longitudinal direction obtained from a flexural test on a FRP pultruded profile is dissimilar from the one obtained from a solid bar coupon of the same profile. But, **(Deskovic *et al.*, 1995)[2]** stated that the elastic moduli obtained from tests on small coupons could lead to reliable values of the same for FRP beams. Due to this diversity on research findings, **(Kumar *et al.*, 2003)[3]**, justified the necessity for conducting more experimental studies on the behaviour of full-size pultruded beams and of coupons extracted from those beams.

The aim of this research is to evaluate the behaviour of GFRP pultruded beams experimentally and with numerical modeling. In the experimental program, two set of beams of same cross section, i.e., 200 × 100 × 8mm, reinforced with CFRP laminates of different orientation and thickness are considered.

II. TIMOSHENKO BEAM THEORY

When beam theory is used for analyzing structural elements, the designer requires to obtain suitable mechanical properties for the selected theory. The option of beam theory depends on various factors, one of which is the degree of anisotropy of the composite material. Composite materials exhibit a longitudinal-to-shear modulus ratio considerably advanced than those found in isotopic materials and this ratio tends to enlarge as the anisotropy degree of the material increases. For this cause shear deformation in the beam will get amplified as the anisotropy degree of the material increases. To account for shear deformation, Timoshenko beam theory provides a

 DOI : 10.18231/2454-9150.2018.0538

better approximation of the real behaviour as compared to the traditional Euler-Beam Theory.

In Timoshenko Beam Theory, the plane sections of the beam are assumed to remain plane, but not anymore normal to the beam neutral axis. The maximum deflection is stated by the expression.

$$\delta = \left(\delta_f + \delta_C\right)_{x=L/2} = \frac{WL^3}{48EI_y} + \frac{WL}{4GK_y 4}$$

$$= \frac{WL^3}{48El_y}\left(1 + \frac{12E}{GK_y\left(L/r\right)^2}\right) \qquad (2.1)$$

Where *W* is the applied vertical load, distributed at two different locations, *L* is the span or the distance between the supports, the area of cross section is termed as *A* and the inertia moment of the section with respect to *y* axis is termed as *I*; the flexural elastic longitudinal modulus for isotropic material is termed as *E*; the shear modulus is termed as *G*, and the shear area coefficient is termed as *K*. For beams made of composite materials, equivalent longitudinal and shear moduli *E* and *G* are required in order to obtain the beam maximum deflection by means of Eqn. 2.1

According to **(Tamizhamuthu 2015)**[4], changes in the fibre orientation can increase the stiffness of the profile. **(Ganesan 2011)**[5] has conducted studies on FRP frames which reveal that shear deformation plays an essential role in calculating the deflection.

Timoshenko beam theory, used to determine the elastic modulus theoretically, had the conclusion that the theoretical values obtained from Timoshenko beam theory have good correlation with the experimental values for beams having at least the ratio of (*l* / *h*) = 40 **(Kolla´r, L. P. 2003,)**[6].

The study conducted by **(Roberts, T. M., and Al-Ubaidi, H. 2002,)**[7] shows that the box and I-beam profiles tested exhibited a large reduction in their flexural stiffness due to their relatively low shear stiffness. The flexural stiffness value (i.e. less than 1% error due to shear deflection) was assessed based on three-point bend test. The performance and failure modes of a glass fibre/polyester profiles were assessed experimentally.

The shear modulus of wider flange beam was found lower than ordinary width I-beam. Lower shear modulus was observed fort wider flange beams and the ratio of *E*/*G* for these beams were found significantly higher than those for the ordinary I-beams. The slenderness ratio (*l*/*r)* of 60 was required for all the beams to have lesser than 10% error in the apparent flexural modulus and a slenderness ratio of 80 for this error drop to 5% **(Lawrence *et al.* 1989)**[8].

It was reported that for intermediate span-to-depth ratios, it resulted in a purely tensile fracture at low loading rates and a purely shear fracture at high loading rates. It was attributed to the fact that the increase in loading rate increases the brittleness of the material and subsequently increases the defect sensitivity leading to a shear failure **(Boukhili *et al.* 1991)**[9].

III. CLASSICAL LAMINATE THEORY (CLT)

The in-plane stiffness properties may be calculated using classical lamination theory, in which the pultruded plate is characterized by its in-plane extensional stiffness coefficients ,A_{ij}. The in-plane engineering stiffness properties may be obtained from standard tests on coupons extracted from the pultruded profile. In this approach, the laminate is supposed to be homogeneous. Since the orthotropic plates, in the pultruded profile, are assumed to be homogeneous on a macro mechanics level, the plate flexural properties can be calculated from their in-plane extensional engineering properties (obtained either from test data or from the in-plane extensional matrix).The orthotropic plate flexural rigidities (the equivalents of *EI* per unit width for a beam) are given as:

$$D_L = \frac{E_L t_p^3}{12(1-\mu_L\mu_T)} \qquad (3.1)$$

$$D_T = \frac{E_T t_p^3}{12(1-\mu_L\mu_T)} \qquad (3.2)$$

$$D_{LT} = \frac{\mu_T E_L t_p^3}{12(1-\mu_L\mu_T)} = \frac{\mu_L E_L t_p^3}{12(1-\mu_L\mu_T)} \qquad (3.3)$$

$$D_s = \frac{G_{LT} t_p^3}{12} \qquad (3.4)$$

Where,D_L,D_T, D_{LT}, and D_S are the longitudinal, transverse, couplings, and shear flexural rigidities andt_p: is the plate thickness. The flexural rigidities relate the plate bending moments (per unit length) to the plate curvatures **(Timoshenko *et al.* 1959)**[10]**.** This notation is frequently used in analytical equations for pultruded profiles.

The in-plane strength properties may be obtained from theoretical calculations or from testing of coupons taken from the laminate, where the theoretical predictions are used, the first ply failure (FPF) is assumed to represent the strength of the laminate. Coupon testing is recommended for obtaining the strength properties for structural design.

1. *Flexural stiffness using CLT*

The flexural and shear stiffnesses can be computed based on the approximate classical laminate theory. Pultruded beams, orthotropic in nature, are estimated to be isotropic, in computing the flexural and shear rigidity. The influences of secondary directions are ignored. (**Nagaraj *et al.* 1997**)[11]. This approximation can be used in rigidity computations.

Pultruded profiles are produced using fibre bundles and fibre mats arranged in layered sequence. Thus, a pultruded

 DOI : 10.18231/2454-9150.2018.0538

profile can be approximated to consist of different layers of fibre laminates of different thickness. A pultruded laminate consists of three stiffness terms, *viz*., extensional stiffness (K_e), bending stiffness (K_b), and bending-extension coupling stiffness (K_{be}). The bending-extension coupling stiffness is zero for symmetric laminates. The extensional stiffness (K_e) and bending stiffness (K_b) terms for a beam's flange and web are given by

Flange:

$$A_f = b\sum_{r=1}^{N} E_r t_r\,;\;\; D_f = b\sum_{r=1}^{N} E_r\left[t_r + \frac{t_{12}^3}{12}\right] \qquad (3.5)$$

Web:

$$A_w = d\sum_{r=1}^{N} E_r t_r\,;\;\; D_w = \frac{d^3}{12}\sum_{r=1}^{N} E_r\, T_r \qquad (3.6)$$

Where b: flange width; d: web depth; E_r: elastic modulus of r^{th} layer in structural coordinate system; t_r: thickness of r^{th} layer and Z_r: distance of middle surface of r^{th} layer from the middle surface of the laminate.

E_r represents the anisotropic modulus. The approximation of a laminate to be isotropic (i.e., E_1=E_2; μ_{12}= μ_{21}; G_{12}=G) eases the computation of E_r required in (3.5, 3.6) and reduces the complexity of beam rigidity computations. The power of secondary directions was not to be significant. Approximating the laminate to be isotropic (E_1=E_2; μ_{12}= μ_{21}) reduces to the form E=E_1

The procedure of theoretical evaluation of flexural stiffness can be explained as below:

Computation of elastic modulus of 900 GSM Bi-axial mat (+45/-45deg)

Thickness of laminate per layer: t; Weight of fibre mat/sq.m: W_f; Density of glass fibre: ρ_f Volume of glass fibre in laminate: F_v=W_f /ρf; Volume of lamina: L_v Volume fraction of fibres: V_f=F_v/L_v;V_m Volume fraction of matrix

Using rule of mixtures the elastic modulus in the direction of fibres

$$E_1 = V_f E_f + V_m E_m \qquad (3.7)$$

Using Mechanics of materials

$$E_2 = \frac{(E_f \times E_m)}{V_f \times E_m + V_m \times E_f} \qquad (3.8)$$

$$G_{12} = \frac{(G_f G_m)}{V_m \times G_f + V_f \times G_m} \qquad (3.9)$$

For +/- 45 deg., the mat is considered to be having two laminates. The elastic modulus can be multiplied by cos 45°. Similarly, the same procedure can be for calculating the properties of carbon mat of 300 GSM density with uni-directional mat. For Bi-directional mat, 50% of carbon fibre in zero deg. and 50% of carbon fibre in 90°. Therefore, the elastic modulus can be accounted for 150 GSM only.

The elastic modulus of glass rovings, the following procedure can be allotted with the following properties:

Length of fibre in m/kg ((1000/(tex/1000)); No. of bundles for each roving layer (n);Width of lamina (W_f); Thickness of each layer (t); Density of fibres(ρ_f); Diameter of fibres D_f =$\left(\sqrt{\frac{1}{\rho Y 9\pi}}\right)$;Volume of fibre$V_f$=$\frac{n\pi D^2}{4bt}$;Volume fraction of matrix ($V_m = 1-V_f$)

Based on the above calculations, the elastic modulus is calculated for bi-axial mat, carbon mat and glass rovings as per the equation described in the subsequent studies.

$$A_f = b(E_1 t_1 + E_2 t_2 + E_3 t_3) \qquad (3.10)$$

$$D_w = \frac{d^3}{12}(E_1 t_1 + E_2 t_2 + E_3 t_3) \qquad (3.11)$$

Similarly, Shear rigidity kAG can be calculated as

$$kAG = d(Gf_1 t_1 + Gf_2 t_2 + Gf_3 t_3) \qquad (3.12)$$

Based on the above calculations the following values are for the six types of beams:

Table 3.1 Theoretical computation of EI and kAG

Beam Type	Flexural Rigidity (EI) N.mm^2	Shear Rigidity(kAG)N
IBBM3MR	6.227×10^{11}	4.039×10^{6}
IBOUCL3MR	7.204×10^{11}	4.039×10^{6}
IBOBCL3MR	6.716×10^{11}	4.039×10^{6}
IBOUOBCL3MR	7.693×10^{11}	4.039×0^{6}
IBTUOBCL3MR	8.67×10^{11}	4.039×10^{6}
IBOUTBCL3MR	8.181×10^{11}	4.039×10^{6}

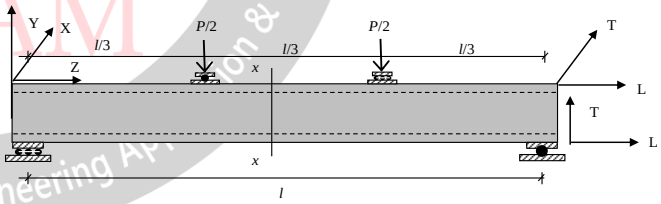

Fig. 3.1 Local and global co-ordinates relationship for a Pultruded Profile

IV. EXPERIMENTAL INVESTIGATIONS

1. Preparation of GFRPI-beams along with CFRP laminates with different fibres orientations

All GFRP I-Beams are manufactured using Pultrusion process as per the ASTM D 4385–2013 standards and are designated as per the fibre orientations. Table 2.1 shows the designations of different beams. The experiment was carried out on six sets of FRP Pultruded I Beams and all the beams of this category are manufactured and tested for a span of 3000 mm. Such beams are supported on simple supports i.e. one end has the roller support and other end is hinged. Along the span direction, at six locations with

 DOI : 10.18231/2454-9150.2018.0538

equal intervals, the flanges of all the beams are restrained laterally for all sets of beams. The first set consists of two FRP pultruded I beams, of conventional type, without any CFRP laminates. It is designated as IBBM3MR

The second set consists of two FRP Pultruded I beams, with one layer of bi-directional mat both in the top and bottom flanges, and spanned over 3m with the flanges which are restrained along the span. The flanges and the interjection between the flanges and web are reinforced with one layer of uni-directional (0°) CFRP laminates of 300 GSM. It is designated as IBOUCL3MR. The thickness of uni-directional laminates come around 0.3 mm.

The third set consists of two FRP Pultruded I beams, with one layer of bi-directional mat all along the outer surface and spanned over 3m with the flanges which are restrained along the span. The flanges and the interjection the between flanges and web are reinforced with one layer of bi-directional (0°/90°) CFRP laminates of 300 GSM. It is designated as IBOBCL3MR. The thickness of the bi-directional laminate is 0.3mm.

The fourth set consists of two FRP Pultruded I beams, with one layer of bi-directional mat all along the outer surface and spanned over 3m with the flanges which are restrained along the span. The flanges and the interjection between the flanges and web are reinforced with one layer of uni-directional and one layer of bi-directional CFRP laminates each of 300 GSM. It is designated asIBOUOBCL3MR. The overall thickness of both the laminate is 0.6mm.

The fifth set consists of two FRP Pultruded I beams, with one layer of bi-directional mat all along the outer surface and spanned over 3m with the flanges which are restrained along the span. The flanges and the interjection between the flanges and web are reinforced with two layers of uni-directional and one layer of bi-directional CFRP laminates each of 300 GSM. It is designated as IBTUOBCL3MR. The overall thickness of the laminate is 0.9mm.

The sixth set consists of two FRP Pultruded I beams, with one layer of bi-directional mat all around the outer surface and spanned over 3m with the flanges which are restrained along the span. The flanges and the interjection between the flanges and web are reinforced with one layer of uni-directional and two layers of bi-directional CFRP laminates. It is designated as IBOUTBCL3MR. The overall thickness of the laminate is 0.9mm

All the pultruded I-beams used in this study have a uniform cross-section and a depth of 200mm. The pultruded I beams are manufactured by Pultrusion process by Meena Fibreglas Industries, Pondicherry, India. Each beam has ECR glass roving's of 4800 Tex (Owen Cornings India, Mumbai) with Isopthalic grade polyester resin (Ashland India, Mumbai). On the outer surface, bi-directional mat of 900 GSM with -45° / +45° direction fibre is used (Seartex India, Mumbai). A curing temperature of 140℃ is maintained during the production. The post curing is done in a 4m long oven, at 120℃ for 4 hours (even though it is specified for profiles made using epoxy resin) to ensure complete cross linking of polymeric chain. Once it is post cured, all the specimens are fine cut to a required length using a diamond coated rotary blade. After the specimens are cut and they are inspected, visually for any defects as per ASTM D 4385 – 2013.

The beams with CFRP laminates require additional surface preparation for applying CFRP laminate. The surface over which the carbon fibre applied is surfaced using a 80 grit coated disc using an angle grinder. The surface preparation is necessary to enable the adequate bonding of carbon fibre over the FRP substrate. Carbon fibre roll form of standard 1m width is cut by means of electrically operated scissors in order to prevent damage to the fibres.

Table 4.1-Beam with different designations for experimental analysis

Sl.No.	Profile of specimen	Type	Flange restraint	Span mm	Number of specimens
1	I -200	IBBM3MR	R	3000	2
2	I -200	IBOUCL3MR	R	3000	2
3	I -200	IBOBCL3MR	R	3000	2
4	I -200	IBOUOBCL3MR	R	3000	2
5	I -200	IBTUOBCL3MR	R	3000	2
6	I -200	IBOUTBCL3MR	R	3000	2

The carbon fibre is cut to the required width and length and is placed over the FRP profile. The epoxy resin is applied manually over the carbon fibre. The first layer is placed over the section, when it is wet, the resin and hardener quantity are mixed and applied over the surface in order to create proper bonding of the laminate. After applying each layer, the metal rollers with serration are rolled over the laminate, to remove the entrapped air. After applying all the layers, the surface is covered with a Mylar film and the surface is squeezed out with a rubber spatula, to remove the excess resin. The beams are allowed to cure overnight and placed in an electric oven for post-curing, at 160℃, for 6 hours. After the beams are removed, the edges are trimmed using an angle grinder. Then, the beams are despatched to the laboratory for testing.

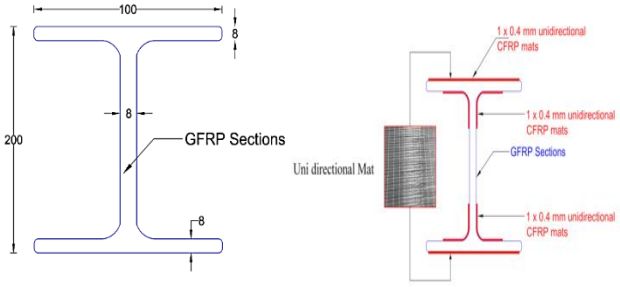

Fig. 4.1 (a) (IBBM3MR) Fig 4.1(b) IBOUCL3MR

 DOI : 10.18231/2454-9150.2018.0538

Fig 4.1 (c) IBOBCL3MR Fig 4.1 (d) IBOUOBCL3MR

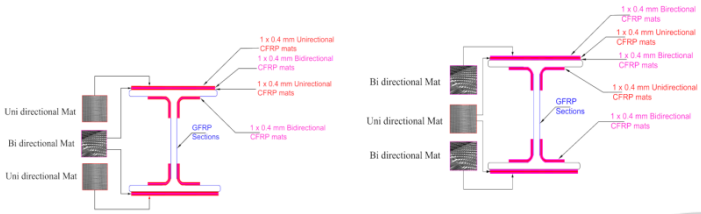

Fig 4.1 (d) IBTUOBCL3MR Fig 4.1 (e) IBOUYBCL3MR

2.Test Specimens

The experimental program is composed of totally twelve beams of 3000mm span. All the twelve beams are tested for static load test. A schematic diagram of the test specimen is shown in Figure 4.4. The various beam parameters that are considered, in the present study, with their designations are presented in Table 2. All the beams are provided with the grid points to locate the loading points and strain measuring positions. Strain gauges are pasted to measure the strains using electrical strain gauges. In the next section, a detailed experimental setup is explained for three and four point bend test conditions.

3. *Test Setup*

A load frame of 500 KN capacity is used for testing the FRP pultruded I beams, strengthened with the CFRP laminates of various fibre orientations. The monotonically increasing static load is used manually through hydraulic jack of 300 kN capacity. The load applied is measured with the proven ring which has a dial gauge. Steel pedestals of size 750mm×750m and 1000mm height (Fig.4.2) are used to support the beams.

Fig. 4.2Loading frame

The supports are specially made to act as hinge and roller at the ends. A spreader beam of steel I-Beam of depth 125mm is used with stiffened steel plates, near the load points, which can transmit the load from the proven ring to the beam.

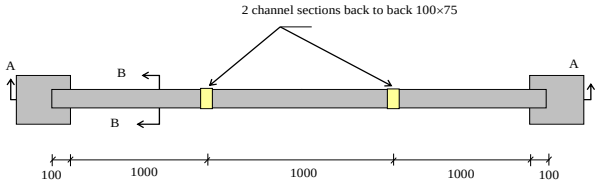

(a) Top view

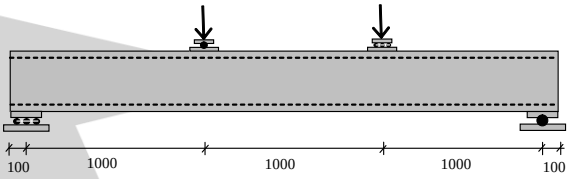

(b) Two point loading

Fig. 4.3 Experimental Test setup

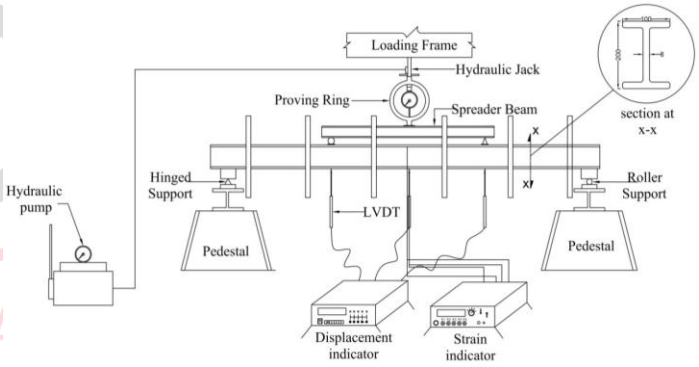

Fig. 4.4 Schematic diagram of I-Beam with lateral restrains (3m)

Additional lateral restrains are given to the flanges along the span direction at six equal intervals of all the I-beams. This frame is fabricated using steel hollow tubes of 40mm × 40mm × 3mm with 470mm spacings. This entire frame is supported on saddle supports and it is isolated from beam supports. The schematic diagram of the frame setup is shown in Fig.4.4. The deformations are measured using the LVDT with a least count of 0.01mm (Linear Variable Displacement Transducer) of 100mm traverse length at three different places, viz., one-third span, mid span and two-third span. A standing adjustable frame is made to hold the LVDT at the required places. All the deformations are measured using a multi-channel digital data acquisition system.

In this experimental setup, the lateral restraints are introduced in order to access its flexural properties exactly. The previous study reveals that open sections are

 DOI : 10.18231/2454-9150.2018.0538

susceptible to lateral torsional buckling. Literature studies revealed that the use of additional lateral restrains can solve the problem of lateral torsional buckling.

4. *Experimental Observations*

All the specimens are tested in the loading frame and the necessary observations are made. The test observations are presented in the form of photographs (Fig.4.5 to Fig 4.9) and graphs in the following sections.

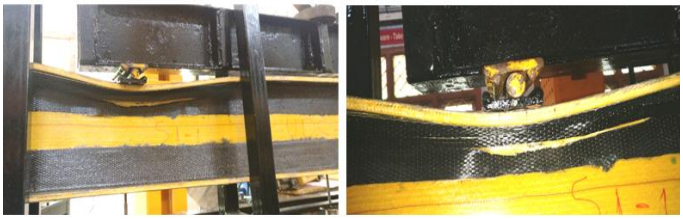

Fig.4.5 Failure of beam (IBOUCL3MR) due to fibre crushing at the flange and web joint in the compression flange

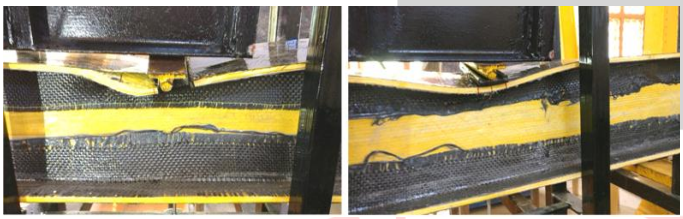

Fig.4.6 Failure of beam (IBOBCL3MR)

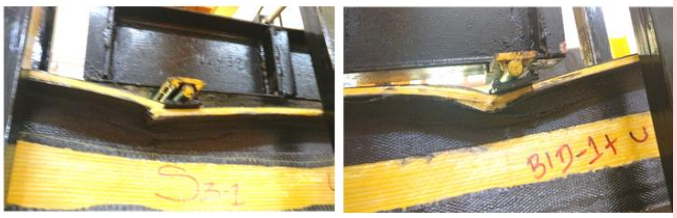

Fig. 4.7 Failure of beam IBOUOBCL3MR (one layer of uni-directional mat and one layer of bi-directional mat)

Fig. 4.8 Failure of beam IBTUOBCL3MR (Two layers of uni-directional mat And one layer of bi-directional mat)

Fig. 4.9 Closer view of failure of beam IBOUTBCL3MR (One layer of uni-directional mat and two layers of bi-directional mat)

The experimental observations are presented in the forms of graphs (Fig.4.10 to Fig.4.17) for various beam parameters and are as follows:

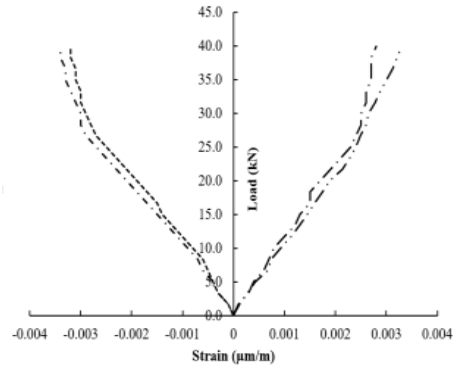

Fig. 4.10 Load versus Strain (IBBM3MR)

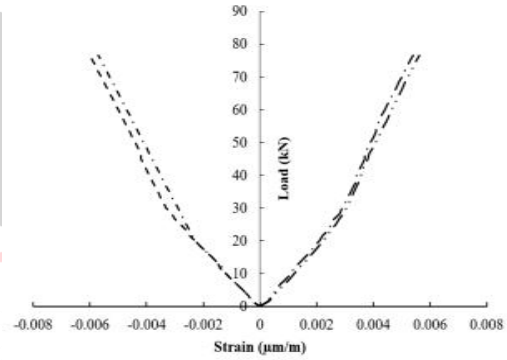

Fig.4.11 Load versus Strain (IBOUCL3MR)

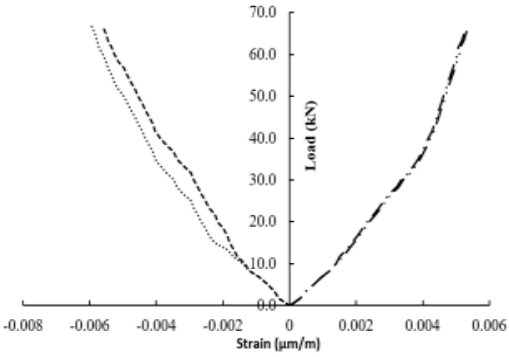

Fig.4.12 Load versus Strain (IBOBCL3MR)

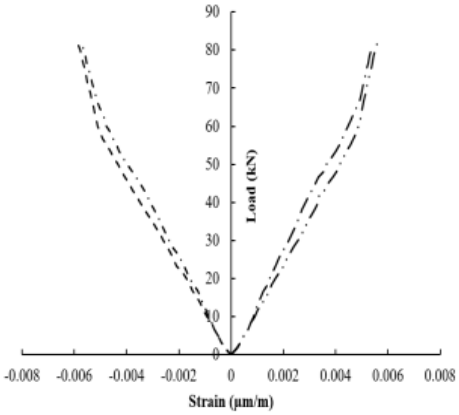

Fig.4.13 Load versus Strain (IBOUOBCL3MR)

 DOI : 10.18231/2454-9150.2018.0538

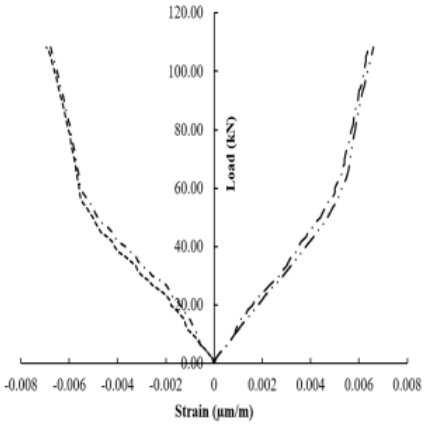

Fig. 4.14 Load versus Strain (IBTUOBCL3MR)

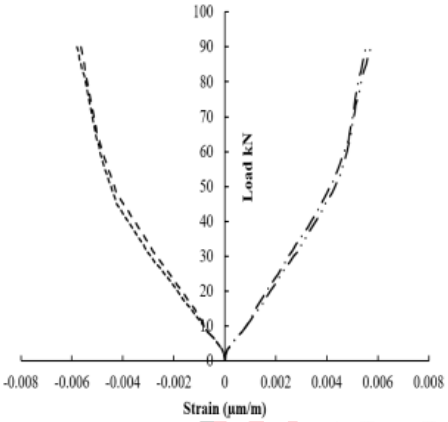

Fig.4.15 Load versus Strain (IBOUTBCL3MR)

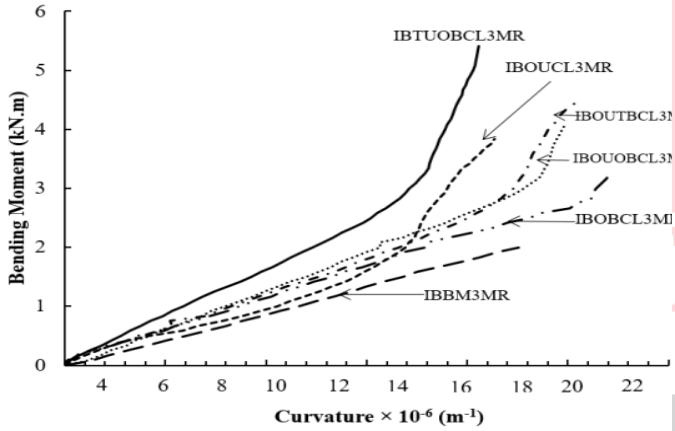

Fig.4.16 Moment versus Curvature

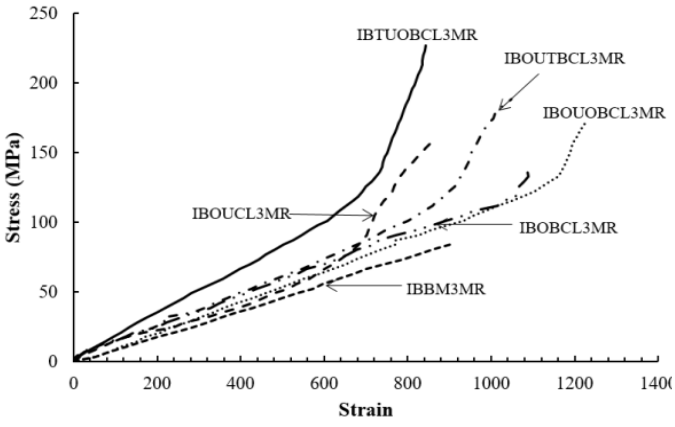

Fig.4.17 Stress versus Strain

V. FINITE ELEMENT MODELLING AND ANALYSIS

1. Modelling of Composites

Composites have orthotropic material properties and each layer has different orthotropic material properties with appropriate orientations. I on this study, the following sequences are adopted for modelling composite and are as follows, Selecting the Proper Element Type ; defining the Layered Configuration; specifying failure criteria for composites; composite modeling and Post-processing Tips

a) Selecting the Proper Element Type

The layered composite materials are modeled using SOLID185 Layered Solid elements. It is defined by eight nodes having three degrees of freedom at each node: translations in the nodal x, y, and z directions...

b) Defining the Layered Configuration

The present research, the different fibre orientations have been considered and are as follows (0^o, 90^o, -45^o, $+45^o$).

c) Specifying Failure Criteria for Composites

The failure criteria are adopted in this study to assess the failure of laminates under the applied loads. Generally, three predefined failure criteria are used and are as follows, Maximum Strain Failure Criterion (it allows nine failure strains); Maximum Stress Failure Criterion (It permits nine failure stresses); Tsai-Wu Failure Criterion (it allows nine failure stresses and three additional coupling coefficients).

d) Composite Modelling and Post-processing concepts

The following general effects to be considered while modeling and post-processing composite elements are as follows, Coupling Effects; Inter-laminar Shear Stresses. Composites exhibit coupling effects, such as coupling between bending and twisting, coupling between extension and bending, etc. For relatively accurate inter-laminar shear stresses at these locations, the element size at the boundaries of the model should be roughly equal to the total laminate thickness.

2. Material Properties Used In Finite Element Modelling

GFRP Pultruded sections are modelled in finite element analysis using properties of unidirectional and bi-directional Chopped Strand Mats (CSM) and CFRP laminates with different fibre orientations. The basic physical and mechanical properties of chopped strand mats and CFRP laminates with different fibre orientations are obtained analytically and from literatures and are presented in Table 5.1, 5.2 & 5.3.The material level properties used in the present study are designated as E_1 (Lamina longitudinal modulus); E_2 (Lamina longitudinal modulus); E_3 (Lamina longitudinal modulus); G_{12} (Lamina shear modulus in plane); G_{13} (Lamina shear modulus in plane); G_{23} (Lamina shear modulus in plane); ν_{12} (Poisson ratio); ν_{13} (Poisson ratio) and ν_{23} (Poisson ratio); and are as shown in Table 5.1; Where a, b, and c are principal material directions.

 DOI : 10.18231/2454-9150.2018.0538

Table 5.1Material properties of Chopped Strand Mat

Fibre Material	Designation	Values
Chopped Strand Mat 	E_1	19000 MPa (Analytical)
	E_2	4000 MPa (Analytical)
	E_3	4000 MPa (Analytical)
	G_{12}	2000 MPa (Analytical)
	G_{13}	2000 MPa (Analytical)
	G_{23}	2000 MPa (Analytical)
	ν_{12}	0.3 (Lit.)
	ν_{13}	0.3 (Lit.)
	ν_{23}	0.3 (Lit.)

Table 5.2 Material properties of Bi-Directional Fibre

Fibre Material	Designation	Values
Bi-Directional 	E_1	23969 MPa (Analytical)
	E_2	4720 MPa (Analytical)
	E_3	4720 MPa (Analytical)
	G_{12}	1923 MPa (Analytical)
	G_{13}	1923 MPa (Analytical)
	G_{23}	1923 MPa (Analytical)
	ν_{12}	0.3(Lit.)
	ν_{13}	0.3(Lit.)
	ν_{23}	0.3(Lit.)

Table 5.3 Material properties of Roving Fibre

Fibre Material	Designation	Values
Roving 	E_1	43295 MPa (Analytical)
	E_2	7530 MPa (Analytical)
	E_3	7530 MPa (Analytical)
	G_{12}	3404 MPa(Analytical)
	G_{13}	3404 MPa(Analytical)
	G_{23}	3404 MPa(Analytical)
	ν_{12}	0.3(Lit.)
	ν_{13}	0.3(Lit.)
	ν_{23}	0.3(Lit.)

Table 5.4Material properties of Bidirectional CFRP Laminates

Fibre Material	Designation	Values
Bidirectional CFRP 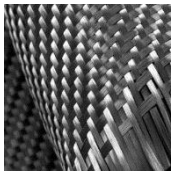	E_1	200078 MPa
	E_2	7313 MPa
	E_3	7313 MPa
	G_{12}	2608 MPa
	G_{13}	2608 MPa
	G_{23}	2608 MPa
	ν_{12}	0.3(Lit.)
	ν_{13}	0.3(Lit.)
	ν_{23}	0.3(Lit.)

Table 5.5Material properties of Unidirectional CFRP Laminates

Fibre Material	Designation	Values
Unidirectional CFRP 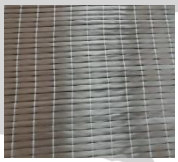	E_1	43000 MPa
	E_2	5000 MPa
	E_3	5000 MPa
	G_{12}	6500 MPa
	G_{13}	6500 MPa
	G_{23}	6500 MPa
	ν_{12}	0.33(Lit.)
	ν_{13}	0.33(Lit.)
	ν_{23}	0.33(Lit.)

Note: Exp – Experimental observation; Lit – Literature

3. Assumptions Made In This Study

The present study is carried out with the following assumptions

a) Full size FRP pultruded I beams are considered for finite element analysis. The boundary conditions adopted in this study are as follows, allowing rotations and displacements along the horizontal axis direction at the one end of the support, rest of the degrees of freedom are restrained. The other end of the support allows rotation but not the displacements along the horizontal axis direction and all other degrees of freedom restrained.

b) Concentrated loads are applied to create pure bending effect similar to experimental setup. The entire flange width is applied uniformly as a line load at the top of the flange. The distance of load on either side of the beam is one-third distance from support. Obviously this loading system provides pure bending effect. It has been proved experimentally.

c) FRP pultruded beams are modelled as three dimensional solid elements; only uni-directional stress-strain relation is adopted. All pultruded member and laminates both GFRP/CFRP are modelled with the same elements.

d) The non-linearity derived from non-linear material models is considered. The result of geometric non-linearity is not considered.

 DOI : 10.18231/2454-9150.2018.0538

4. Finite Element Modelling

In the present study, the Finite element (FE) models are developed using ANSYS 15.0. The properties of GFRP pultruded beams are tabulated. The regular meshing concept is utilized to model the pultruded sections and the laminates. Initially all predefined nodes are created then linked with nodes of finite elements. This is utilized for further nodes by copying the entire model for subsequent node increments. Having completed the geometry, the entire nodes and elements are compressed to overcome the problem of redundant nodes. The support conditions adopted in this study mimic the experimental setup, i.e. one end is on roller and other end is hinged. Roller end allows U_z, R_x degrees of freedom and hinged end allows R_x degree of freedom. Lateral supports are introduced near the flanges at six locations as shown in Fig. 5.1. Such lateral restraints prevent displacements i.e.U_y degree of freedom is prevented. All external loads are applied through nodes of the finite element near the top flanges. The vertical deflections are measured at the supports and at mid span bottom flange in-order toverify the experimental results. The constitutive model for the FRP pultruded sections are considered as orthotropic and linear–elastic. The classical lamination theory is used along with the rule of mixtures for assessing the elastic properties. Most of the elements aspect ratios adopted in this study are well within the limits. Finite elements convergence study is also carried to verify the convergence of the number of elements used. The Classical Lamination Theory (CLT) and the Rule of Mixtures were utilized for estimating all elastic properties, with the exception of the shear modulus for which the Halphin and Tsai equations are adopted. The profile is made of fibre glass rovings bonded in a polyester matrix, with a fibre volume fraction of 68%,with external laminates made of bi-axial fibreglass mats.

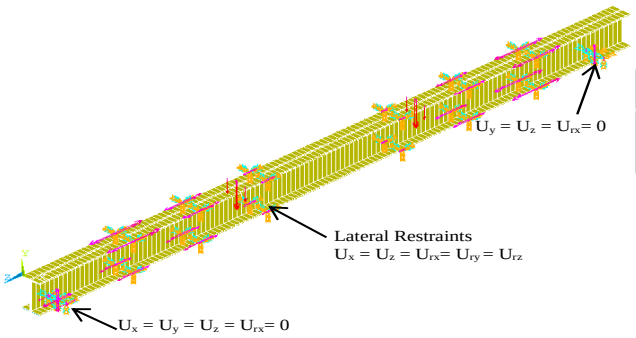

Fig 5.1 FE Cartesian coordinate system, and mesh with displacementend boundary conditions

5. *Finite Element Analyses*

This study uses Timoshenko beam theory to analyze the FRP pultruded I-beams subjected to four point bending and results are verified with experimental values. The nonlinear analysis procedure uses Newton-Raphson equilibrium iterations for updating the model stiffness. The convergences at the end of each load increment are within tolerance limits. The load step sizes are done automatically and it forecasts and controls load step sizes. Based on the earlier solution history and the physics of the models, if the convergence behaviour is smooth, the load additionis increased to a selected maximum load step size by automatic time stepping. If the convergence behaviour is sudden, the load increment is bisected by automatic time stepping, until it is equal to a particular minimum load step size. The maximum and minimum load step sizes are required for the automatic time stepping. These analyses are carried outfor modelling and analysis with high end system configuration with an integrated environment. (Sivagamasundari2006, Deiveegan 2010, Saravanan 2011, ANSYS Manual). The results are also compared with experimental observations.

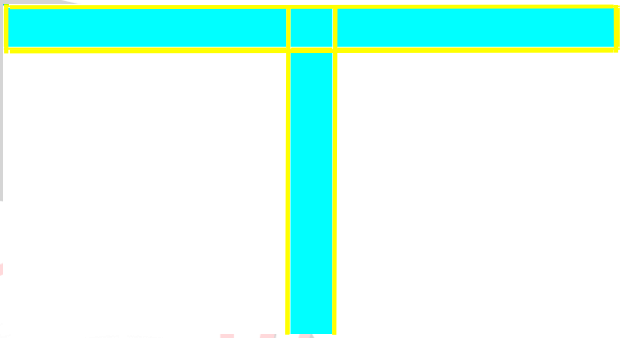

Fig. 5.2 Cross section

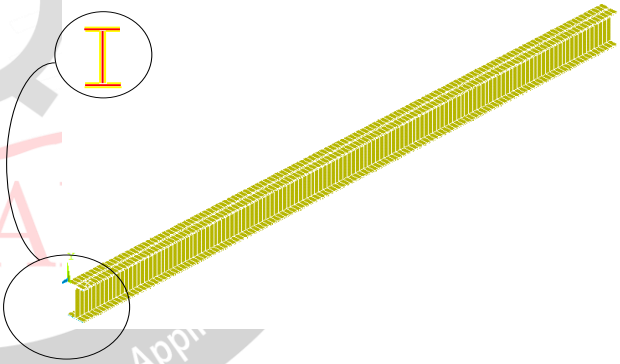

Fig. 5.3 Finite Element Model of FRP I Beam with bi-directional Fibre mat its outer skin (IBBM3MR)

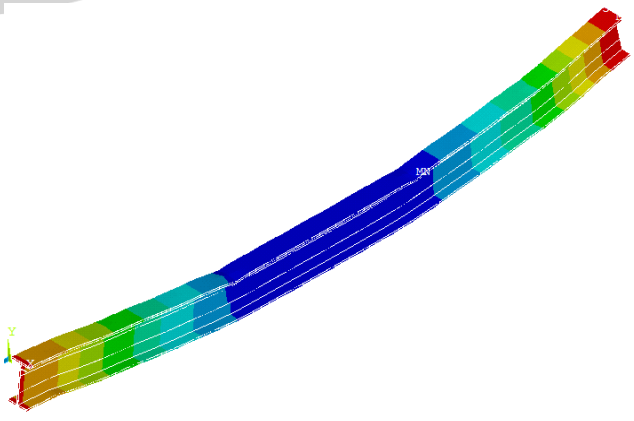

Fig.5.4 Typical Displacement Contour of I Section with Bidirectional mat Fibre on Extreme Layer (IBOUCL3MR)

 DOI : 10.18231/2454-9150.2018.0538

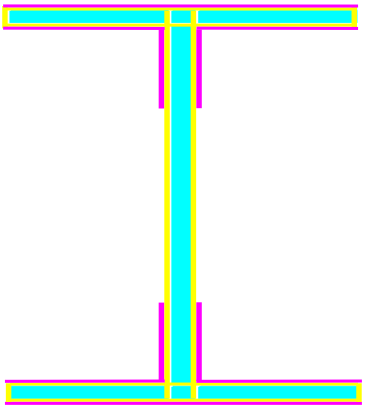

Fig. 5.5 Cross section

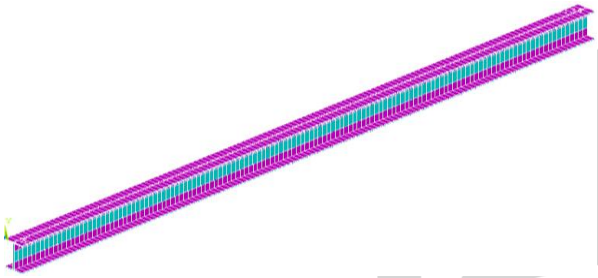

Fig. 5.6 I section with one layer BidirectionalCFRP mat (IBOBCL3MR)

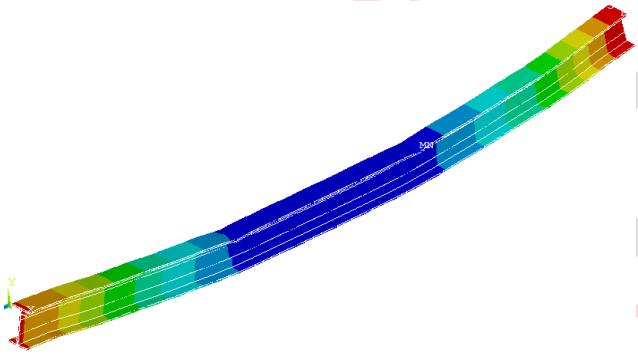

Fig. 5.7 Typical Displacement Contour of I Section with Bidirectional mat Fibre on Extreme Layer (IBOUCL3MR)

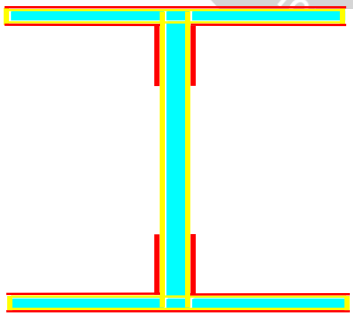

Fig.5.8 Cross section

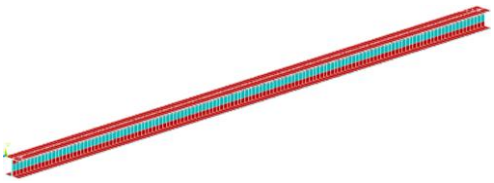

Fig. 5.9 I section with one layer Unidirectional CFRP mat (IBOUCL3MR)

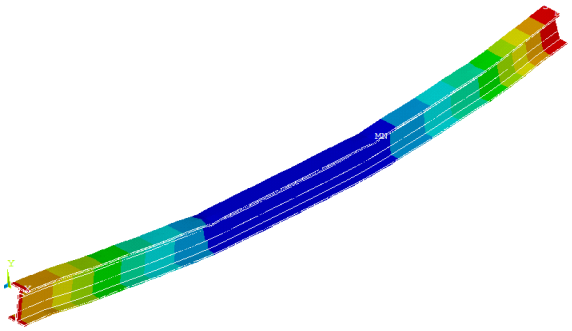

Fig.5.10 Typical Displacement Contour of I section with one layer Unidirectional CFRP mat

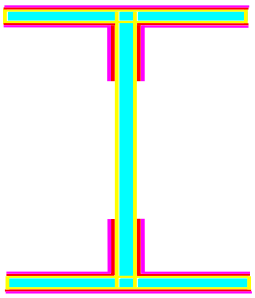

Fig. 5.11 Cross section

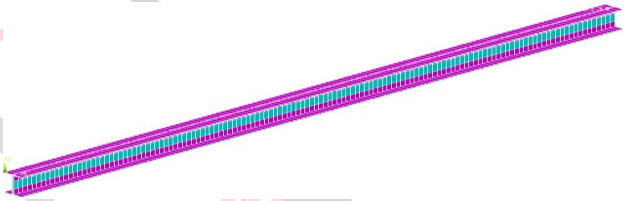

Fig.5.12 Modelling of Extreme Layer of I – Beam with Bi-Directional Fibre (IBOUOBCL3MR)

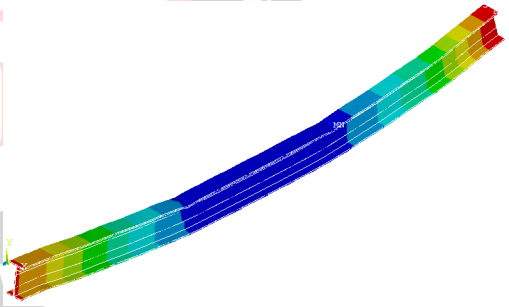

Fig.5.13 Typical Displacement Contour Of I – Beam with Bi-Directional Fibre

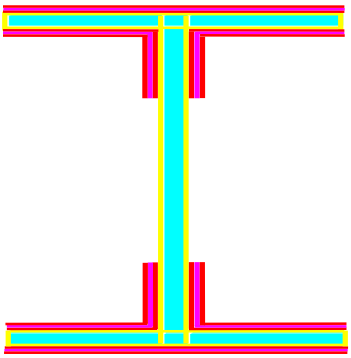

Fig. 5.14 Cross section

 DOI : 10.18231/2454-9150.2018.0538

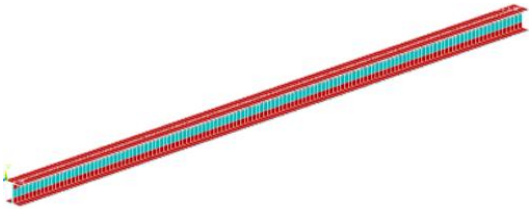

Fig. 5.15 Modelling of Extreme Layer of I – Beamwith Bi-Directional Fibre(IBTUOBCL3MR)

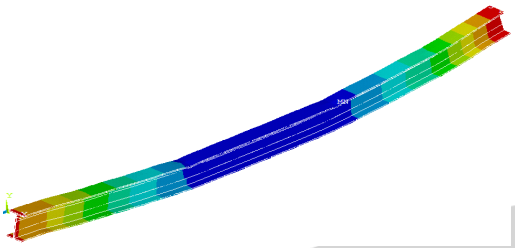

Fig.5.16 Typical Displacement Contour of I – Beam with Bi-Directional Fibre

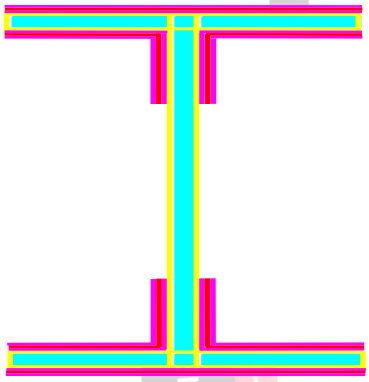

Fig. 5.17 Cross section

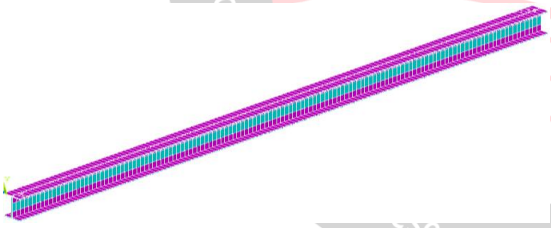

Fig. 5.18 Modelling of Extreme Layer of I – Beam with Bi-Directional Fibre (IBOUTBCL3MR)

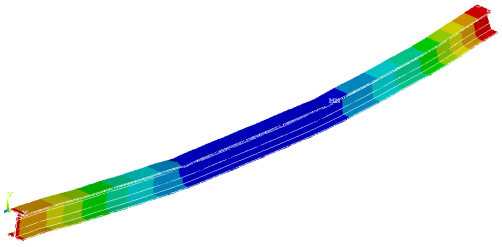

Fig.5.19 Typical Displacement Contour of I – Beam with Bi-Directional Fibre

From this study, the following observations are made in the form of load verses deflection graphs (Figs. 5.20 to 5.25) and few contours are also depicted for the different parametric conditions in Figs. 5.4, 5.7, 5.10, 5.13, 5.16, 5.19.

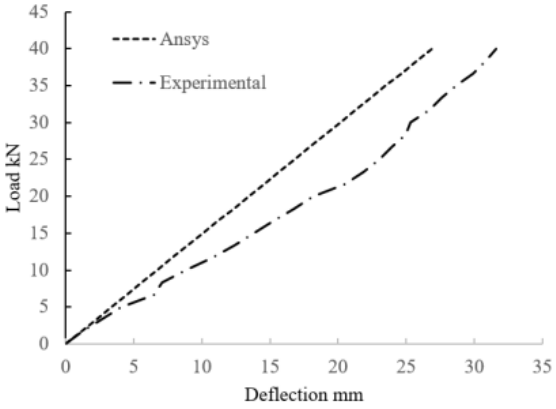

Fig. 5.20 Load versus Deflection (IBBM3MR)

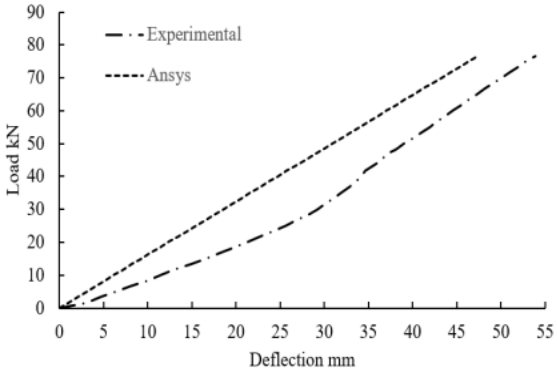

Fig. 5.21 Load versus Deflection (IBOUCL3MR)

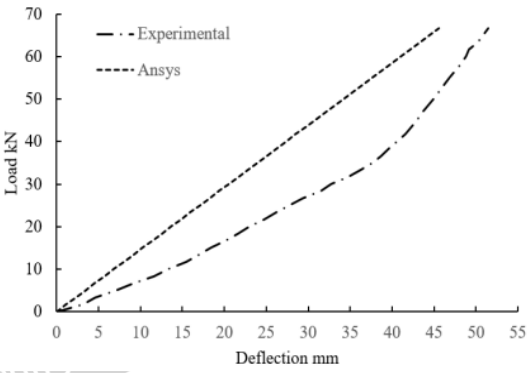

Fig. 5.22 Load versus Deflection (IBOBCL3MR)

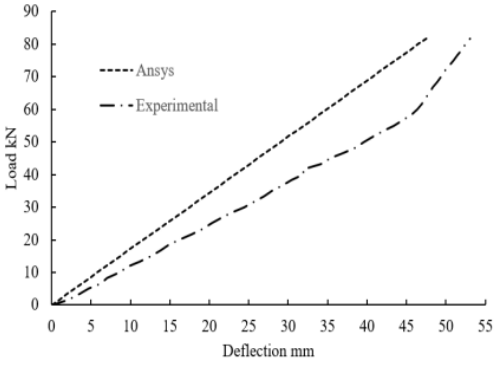

Fig. 5.23 Load versus Deflection (IBOUOBCL3MR)

 DOI : 10.18231/2454-9150.2018.0538

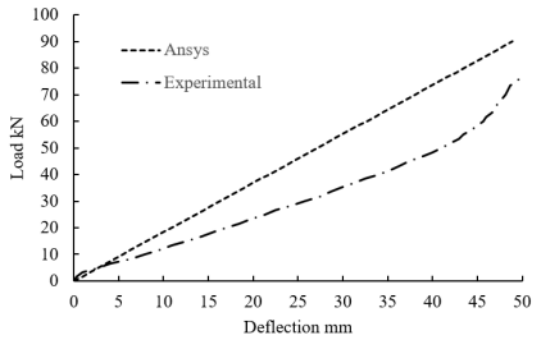

Fig. 5.24 Load versus Deflection (IBOUOBCL3MR)

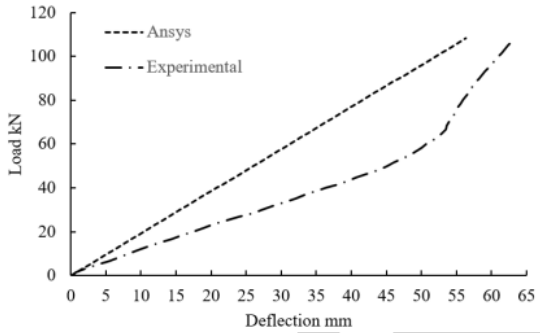

Fig. 5.25 Load versus Deflection (IBTUOBCL3MR)

VI. CONCLUSION

A static non-linear analysis is carried to develop trustworthy and computationally efficient finite element models for the analysis of FRP Pultruded I-beams under two point loading conditions. The finite element model developed in this study is used to replicate the static experimental tests performed. The following comparisons are made: load-strain plots upto failure for various parametric conditions. The results of the finite element study are compared with experimental study and suitable recommendations are made for the type of modeling and method of analysis.

1) The general behaviour of the finite element models signified by the load-displacements plots show excellent agreement with the experimental data. However, the finite element models illustrate higher loads than the experimental study both in linear and non-linear ranges. This is credited to higher stiffness attributed from shear energy accumulation.
2) The numerical solutions are executed with the present model, by using the Timoshenko approach for composites in bending which is then compared with the experimental curve.
3) Discrete finite element model establish to be computationally simple and better depiction of the actual behaviour of the FRP pultruded I-beams for various parametric conditions. But the results show a similar trend as that of the experimental approach despite the buckling trend. Experimental results difficult to trace the buckling part
4) The result specifies that the effect of flexural strains shows an excellent agreement with the experimental results in the earlier division of the load versus deflection curve because this system reduces the shear stiffness.
5) The load-strain plots for particular locations from the finite element analysis displays fair agreement with the experimental data. The load-compressive strain plots from the experimental study have fine agreement with those from the finite element analysis. The strain values range from 0.0037 to 0.0063 for experimental study.
6) The deflection for the finite element examine are lesser than the experimental results by 15% to 20% (Fig. 5.20-5.25).
7) The load-strain plots for selected locations i.e. at the middle of the span near the bottom flange from the finite element analysis show fair accord with the experimental data. The load-compressive strain plots (at mid span at the centre of the top face) from the experimental study have good agreement with those from the finite element analysis (Figs 5.4, 5.7, 5.10, 5.13, 5.16, 5.19).

Comparison of load–displacement curves obtained numerically and experimentally, shows a very good approximation of the FEM and TBT in relation to the experiments, for all beams. It can thus be concluded that in the design of beams with FRP pultruded I beams, the TBT with mechanical properties estimated by CLT can be used to evaluate the beam stiffness and verify deflections for service loads. However, for estimation of the mechanical properties, the individual properties of fibres and resin, the fibre volume fraction, and the composition of all laminates should be reasonably accurate.

REFERENCES

[1] **Bank, L.C.** (1989a), Flexural and shear moduli of full-section fibre reinforced plastic (FRP)pultruded beams, *Journal of Testing and Evaluation*, Vol. 17, No. 1, pp. 40–45
[2] **Deskovic *et al.*,** 1995, Innovative Design of FRP Combined with Concrete Long- Term behaviour, *Journal Of Structural Engineering, Vol 121, Issue 7.*
[3] **Kumaran,G., D.Menon and K.Khrishnan Nair,** (2003 a),Reliability Analysis and Design of PSC rail track sleepers, *Proceedings of the international conference on applications of statistics and probability in Civil Engineering*, San Francisco, California, USA, July 6-9.
[4] **Tamizhamuthu .S,** Experimental and analytical investigations on the flexural behaviour of FRP pultruded I beam sections. M.E Structural Engineering Thesis report, AU, A.Nagar, India. 2015.
[5] **Ganesan .G,** Experimental study on the behaviour of telecommunication tower using FRP pultruded sections. M.E Structural Engineering Thesis report, AU, A.Nagar, India, 2011.
[6] **Kolla´r, L. P**. (2003), Local buckling of fibre reinforced plastic composite structural members with open and closed cross sections, *Journal of Structural Engineering*, Vol. 129,No. 11, pp. 1503–1513.
[7] **Roberts, T. M., and Al-Ubaidi, H**. (2002), Flexural and torsional properties of pultruded fibre reinforced plastic I-

 DOI : 10.18231/2454-9150.2018.0538

profiles, *Journal of Composites for Construction*, Vol. 6,No. 1, pp. 28–34.

[8] **Bank, L. C.** (1989b), *Properties of Pultruded Fibre Reinforced Plastic* (*FRP*) *Structural Members*, Transportation Research Record 1223, National Research Council, Washington, DC, pp. 117–124.

[9] **Boukhili *et al.* 1991**Investigation of water absorption in pultruded composites containing fillers and low profile additives, Journal of Polymer Composites, Vol : 28, Issue: 3

[10] **Nagaraj, V., and GangaoRao, H. V. S**. (1997), Static behavior of pultruded GFRP beams, *Journal of Composites for Construction*, Vol. 1, pp. 120–129.

[11] **Timoshenko, S., and Woinowsky-Krieger, S**. (1950), *Theory of Plates and Shells*, McGraw-Hill, New York.

[12] **Bakis, C. E., Bank, L. C., Brown, V. L., Cosenza, E., Davalos, J. F., Lesko, J. J., Machida, A., Rizkalla, S. H., and Triantafilliou, T. C.** (2002), Fibre-reinforced polymer composites for construction: state-of-the-art review, *Journal of Composites for Construction*, Vol. 6, No. 2, pp. 73–87.

[13] **Bank, L.C.** (1987), Shear coefficients for thin-walled composite beams, *Composite Structures*, Vol. 8, pp. 47–61.

[14] **Bank, L. C., and Melehan, T. P.** (1989), Shear coefficients for multicell thin-walled composite beams, *Composite Structures*, Vol. 11, pp. 259–276.

[15] **Bank, L. C., and Mosallam, A. S.** (1992), Creep and failure of a full-size fibre reinforced plastic pultruded frame, *Composites Engineering*, Vol. 2, pp. 213–227.

[16] **Bank, L. C., Gentry, T. R., and Nadipelli, M.** (1996a), Local buckling of pultruded FRP beams: analysis and design, *Journal of Reinforced Plastics and Composites*, Vol. 15, pp. 283–294.

[17] **Bank, L. C., Nadipelli, M., and Gentry, T. R**. (1994b), Local buckling and failure of pultruded fibre-reinforced plastic beams, *Journal of Engineering Materials and Technology*, Vol. 116, pp. 233–237.

[18] **Bank, L. C., Yin, J., and Nadipelli, M**. (1995a), Local buckling of pultruded beams: nonlinearity, anisotropy and in homogeneity, *Construction and Building Materials*, Vol. 9, No. 6, pp. 325–331.

[19] **Bank, L.C.,** (2006), Composites for Construction: Structural Design with FRP Materials. *Wiley & Sons, Inc*. ISBN: 978-0-471-68126-7

[20] **Barbero, E. J.** (1999), *Introduction to Composite Materials Design*, Taylor & Francis, Philadelphia.

[21] **Bedford** (2005), *Bedford Reinforced Plastics Design Guide*, Bedford Plastics, Bedford, PA; www.bedfordplastics.com.

[22] **CEN** (2002a), *Reinforced Plastics Composites: Specifications for Pultruded Profiles*, Part 1: Designation; Part 2: Method of Test and General Requirements; Part 3: Specific Requirements, EN 13706, Comite´ Europe´en de Normalisation, Brussels, Belgium.

[23] **CEN** (2002b), *Eurocode 1: Actions on Structures*, Comite´ Europe´en de Normalisation, Brussels, Belgium.

[24] **Chambers, R. E.** (1997), ASCE design standard for pultruded fibre-reinforced plastic (FRP) Structures, *Journal of Composites for Construction*, Vol. 1, pp. 26–38.

[25] **Cowper, G. R.** (1966), The shear coefficient in Timoshenko's beam theory, *Journal of Applied Mechanics*, Vol. 33, pp. 121–127.

[26] **Creative Pultrusions** (2004), *The Pultex Pultrusion Global Design Manual*, 4th ed. Creative Pultrusions, Alum Bank, PA; www.creativepultrusions.com.

[27] **CTI** (2003), *Fibreglass Pultruded Structural Products for Use in Cooling Towers*, STD-137, Cooling Technology Institute, Houston, TX.

[28] **Daniel, I. M., and Ishai, O**. (1994), *Engineering Mechanics of Composite Materials*, Oxford University Press, New York.

[29] **Davalos, J. F., and Qiao, P.** (1997), Analytical and experimental study of lateral and distortional buckling of FRP wide-flange beams, *Journal of Composites for Construction*, Vol. 1, pp. 150–159.

[30] **Deiveegan, A. and Kumaran, G.** (2009) "Reliability Based Analysis of Concrete Columns Reinforced Internally with GFRP Reinforcements," *Proceedings of International conference on Recent Developments in Structural Engineering-RDSE*, 217-224, India, 2007.

[31] **Erki, M. A.** (1995), Bolted glass-fibre-reinforced plastic joints, *Canadian Journal of Civil Engineering*, Vol. 22, pp. 736–744.

[32] **Eurocomp** (1996), Structural design of polymer composites, *Eurocomp Design Code and Handbook* (ed. J. Clarke), E&FN Spon, London.

[33] **Fibreline** (2003), *Fibreline Design Manual*, Fibreline, Kolding, Denmark; www.fibreline.com.

[34] **Goldsworthy, B.** (1954), The continuous extrusion of RP, *Proceedings of the 9th SPIRPD Conference*, Chicago, February 3–5, Section 13.

[35] **Kolla´r, L. P**. (2002), Buckling of uni-directionally loaded composite plates with one free and one rotationally restrained unloaded edge, *Journal of Structural Engineering*, Vol. 128, No. 9, pp. 1202–1211.

[36] **Kolla´r, L. P**. (2003), Local buckling of fibre reinforced plastic composite structural members with open and closed cross sections, *Journal of Structural Engineering*, Vol. 129,No. 11, pp. 1503–1513.

[37] **Kolla´r, L. P., and Springer, G. S**. (2003), *Mechanics of Composite Structures*, Cambridge University Press, Cambridge.

[38] **Lackey, E., and Vaughan, J.** (2002), Resin fillers and additives, *Composites Fabrication*, March, pp. 12–17, 36.

[39] **Macgregor, J.G., S. Mirza and B .Ellingwood (1983)** Statistical analysis of Resistance of reinforced and pre-stressed concrete members**,** *Journal of American Concrete Institute*, ACI, 80(3), 167-176.

[40] **Melchers, R.E., (1999),** Structural Reliability: Analysis

 DOI : 10.18231/2454-9150.2018.0538

and Prediction, *John Wiley and Sons*, Chichester.

[41] **Meyer, L. S.** (1970), Pultrusion, *Proceedings of the 25th Annual Technical Conference*, Society for the Plastics Industry, New York, Section 6-A, pp. 1–8.

[42] **Meyer, R. W**. (1985), *Handbook of Pultrusion Technology*, Chapman & Hall, London.

[43] **Meyer, R. W**. (1992), Lateral torsional buckling of a pultruded I beam, *Composites*, Vol. 23, pp. 81–92.

[44] **Meyer, R. W.** (1993), Short- and long-term structural properties of pultruded beam assemblies fabricated using adhesive bonding, *Composite Structures*, Vol. 25, pp. 387–395.

[45] **Meyer, R. W**. (2001), Analysis and design of connections for pultruded FRP structures, in *Composites in Construction: A Reality*, ASCE, Reston, VA, pp. 250–257.

[46] **Mottram, J. T., and Zheng, Y.** (1999b), Further tests on beam-to-column connections for pultruded frames: flange-cleated, *Journal of Composites for Construction*, Vol. 3, pp. 108–116.

[47] **Nowak, A. S. and K. R Collins** (2000), Reliability of Structures, *McGraw-Hill*.

[48] **Pecce, M., and Cosenza, E**. (2000), Local buckling curves for the design of FRP profiles, *Thin-Walled Structures*, Vol. 37, pp. 207–222.

[49] **Prabhakaran, R., Razzaq, Z., and Devera, S**. (1996), Load and resistance factor design (LRFD) approach to bolted joints in pultruded structures, *Composites: Part B*, Vol.27B, pp. 351–360.

[50] **Ranganathan.R.(**1999) Structural Reliability Analysis and Design, *Jaico Publishing House*, NewDelhi

[51] **Razzaq, Z., Prabhakaran, R., and Sirjani, M. M**. (1996), Load and resistance factor design (LRFD) approach for reinforced-plastic channel beam buckling, *Composites: Part B*, Vol. 27B, pp. 361–369.

[52] **Smith, C., McEwen, S., and Tillson, J.** (1998), The effect of different continuous strand mats on Pultrusion property performance, *Proceedings of the International Composites Expo*, Nashville, TN, January 19–21, Section 19A, pp. 1–10.

[53] **Starr, T. (ed.),** (2000), *Pultrusion for Engineers*, CRC Press, Boca Raton, FL.

[54] **Strongwell** (2002), *Strongwell Design Manual* (CD ROM), Strongwell, Bristol, VA; www.strongwell.com.

[55] **Timoshenko, S., and Gere, J.** (1961), *Theory of Elastic Stability*, 2nd ed., McGraw-Hill, New York.

[56] **Turvey, G. J.** (1996), Effects of load position on the lateral buckling response of pultruded GRP cantilevers: comparisons between theory and experiment, *Composite Structures*, Vol. 35, pp. 33–47.

[57] **Wang, Y., and Zureick, A**. (1994), Characterization of the longitudinal tensile behavior of pultruded I-shape structural members using coupon specimens, *Composite Structures*, Vol. 29, pp. 463–472.

[58] **Yeh, H. S., and Yang, S. C**. (1997), Building a composite transmission tower, *Journal of Reinforced Plastics and Composites*, Vol. 16, No. 5, pp. 414–424.

[59] **Yoon, S. J., Scott, D. W., and Zureick, A.** (1992), An experimental investigation of the behavior of concentrically loaded pultruded columns, in *Advanced Composite*

[60] **Zureick, A.** (1998), FRP pultruded structural shapes, *Progress in Structural Engineering and Materials*, Vol. 1, No. 2, 143–149.

[61] **Zureick, A., and Scott, D**. (1997), Short-term behavior and design of fibre-reinforced polymeric slender members under axial compression, *Journal of Composites for Construction*, Vol. 1, pp. 140–149.

[62] **Zureick, A., and Steffen, R**. (2000), Behavior and design of concentrically loaded pultruded angles struts, *Journal of Structural Engineering*, Vol. 126, pp. 406–416.

 DOI : 10.18231/2454-9150.2018.0538